ISSN 0023-1584, Kinetics and Catalysis, 2012, Vol. 53, No. 6, pp. 648–664. © Pleiades Publishing, Ltd., 2012.
Published in Russian in Kinetika i Kataliz, 2012, Vol. 53, No. 6, pp. 690–707.

A Detailed Chemical Kinetic Mechanism for Methanol Combustion in Laminar Flames[1]

S. Hamdane, Y. Rezgui, and M. Guemini

Laboratoire de Chimie Appliquée et Technologie des Matériaux, Université d'Oum ElBouaghi, Algérie

e-mail: m_guemini@yahoo.fr

Received September 27, 2011

Abstract—On the basis of existing detailed kinetic schemes a general and consistent mechanism of the oxidation of methanol was compiled for computational studies covering a wide range of lean to rich flames. The proposed model, featuring 21 species and 115 reactions, has been validated using three data sets and the computed reactants, products and intermediates mole fractions. This scheme was compared to those by Held–Dryer, Egolfopolous and Pauwels under the same conditions. The developed mechanism predicts well the concentrations of the major reactants, intermediates, and products at all the studied equivalence ratios and it gives the best calculated values, as compared to the other used models, as well. The production rates analysis of selected species allowed the identification of the major formation and depletion pathways. A reaction path analysis snowed that the main channels in methanol consumption involved H, OH and O attack and the resulting radicals CH_2OH and CH_3O produced formaldehyde.

DOI: 10.1134/S0023158412060055

Oxygenated hydrocarbons play an important role as fuels in combustion, as well as in industrial processes and environmental chemistry. Methanol, which is the simplest alcohol, is a clean renewable fuel with a large part of useful energy and is in great demand as an intermediate source of energy, particularly in automobiles, fuel cells, space heating, electric power generation, a chemical and so on [1]. In addition, due to environmental considerations, methanol is a leading candidate being considered to extend and replace methyl tertiary butyl ether, used as an additive in petrol to increase the oxygen content. However, the likelihood of the methanol implementation in these capacities requires a higher level of understanding and knowledge of the oxidation processes.

Oxidation of methanol has been studied at high temperatures in shock tubes [2–5], jet-stirred reactors [6], and flames [7–9], and in the low-to-medium temperature range in batch reactors [10], flow reactors [11–14], and supercritical water [15–17]. It is well known that the development of detailed chemical kinetic models allows interpretation of the kinetic behavior of the experiments used in their validation. Thus, in order to describe methanol experiments in term of reaction mechanism containing elementary steps, a few detailed models have been proposed and discussed. Westbrook and Dryer [18] developed a mechanism for methanol oxidation, applicable to temperatures in the range 1000–2200 K, pressures of 1–5 atm, and equivalence ratios of 0.05–3.0. This model has been applied in a number of studies on methanol to simulate the results (ignition delay times, flame velocities, and species concentrations) of many different experiments. However, this work was hampered by a lack of elementary rate constant and reaction path information. Dove and Warnatz [19] proposed a new mechanism containing 15 species and 40 elementary reactions which was used by Pauwels et al. [20] to simulate their stoichiometric methanol-air flame data. It was found that the model predicted CO and H_2 concentrations larger than those measured whereas the reverse holds for the CO_2 profiles. As new information on methanol oxidation (new rate constants and a consistent set of thermochemical parameters) became available, the Westbrook and Dryer model was modified by Norton and Dryer [11]. A better agreement with the flow-reactor data has been observed, and the importance of the hydroperoxyl radical (HO_2) to methanol oxidation kinetics has been noticed. A more recent methanol oxidation mechanism was constructed by Egolfopoulos, Du and Law [21]. The authors have found that their model predicted excellently both the laminar flame speed and atmospheric-pressure flow-reactor data set [22]. However, the ability of the model to predict the Bowman's shock-tube ignition delay measurements has been questioned [3]. Recently, Held and Dryer, using a hierarchical procedure, have developed a detailed comprehensive kinetic model that includes advances in chemical kinetic rate and thermochemical information as well as validation data sources [23]. It was found that this model satisfactorily reproduces measurements from four different types of experiments (static reactors, flow reactors, shock-tubes and lami-

[1] The article is published in the original.

nar flames) over a wide range of temperature, pressure, and equivalence ratio. However, in premixed flames, it does not reproduce H and H_2 profiles with a good accuracy. These findings suggest that despite the extensive efforts devoted to methanol oxidation, important aspects of its chemistry are still unresolved especially at high temperatures.

To gain a more detailed understanding of methanol oxidation in the low pressure, high temperature regime, a detailed chemical kinetic model has been constructed and validated by comparison to data and models available in the literature.

MODEL DEVELOPMENT PROCEDURE

Based on the H_2, CO, CH_2O, and CH_3OH combustion chemistry, a detailed mechanism for methanol oxidation was hierarchically developed. The reaction submechanisms of each of the above mentioned species used here were based on previously published studies. The mechanism was developed by evaluating the importance of each species and reaction step for the chemical processes by sensitivity analysis. Unimportant reaction species and steps were judiciously removed.

For each elementary reaction, the overall rate constants proposed in the literature were tested and their influence on the molar fractions profiles of stable and unstable species in the various studied flames was checked. For each elementary reaction, the constant rate giving the best agreement between experimental and modelled profiles for different species was selected. On the other hand, it was found that C_2 submechanism as well as CH and CH_2 (singlet and triplet states) reactions had no significant effects on stable and unstable species concentration profiles so they were not taken into account in our model. Same trends were reported by several authors [24–26] for methanol combustion over almost all conditions of practical interest. Taking these observations into account, a detailed homogeneous gas-phase kinetic mechanism containing 21 species involved in 115 elementary reactions has been developed for the CH_3OH oxidation.

COMPUTATIONAL PROCEDURE

Computations were carried out using the Sandia laminar one-dimensional premixed flame code (PREMIX) [27] of the Chemkin package [28]. The PREMIX code computes concentration profiles for a burner-stabilized premixed laminar flame using the cold mass flow rate through the burner, feed gas composition, pressure, and an initial guess of the solution profile as input. To compensate for the cooling effect of the flame by the probe and the burner, the experimentally determined temperature profile were used as input [7, 20]. The reverse reaction rates were calculated using equilibrium constants and species thermodynamic data taken from the literature [29–34] or theoretically computed.

MECHANISM VALIDATION

Among the various experimental studies which have been conducted on low pressure methanol flames using the flat-flame burner technique, the experimental data reported by Vandooren and Van Tiggelen for lean methanol flames [7], Pauwels et al. for stoichiometric methanol flames [20] and Bradley et al. for rich methanol flames [33] were modelled herein using our proposed model. The calculated data were then compared to the numerical predictions obtained by using the schemes reported by Held and Dryer [23], Pauwels et al. [20] and Egolfopolous et al. [21] under the same conditions.

Held and Dryer mechanism, noted as **HD model**, contains 40 species involved in 96 reversible reactions, whereas Pauwels et al. [20] mechanism, noted as **Pauwels model**, is a scheme based on the mechanism developed by Dove and Warnatz [19] which contains 15 species and 40 elementary reactions. In this model, most rate constants have been updated according to the new estimation of Warnatz [35] except for reactions $H + O_2 + M \rightarrow HO_2 + M$ and $CH_2O + HO_2 \rightarrow CHO + H_2O_2$ which have been taken from the Lawrence Livermore laboratory data base revised in 1985 [20]. For the three body reactions, Pauwels and coworkers have assigned equal collision efficiencies to all species and have chosen the recommended rate value for $[M] = [N_2]$ or [Ar]. Finally, Egolfopolous et al. [21] mechanism, noted as **Egolfopolous model**, is a scheme with 30 species involved in 171 reversible reactions.

Validation on Lean Flames

In their study, Vandooren and Van Tiggelen [7] used the molecular beam sampling technique, coupled with mass spectrometric detection to measure the concentrations of both stable species and radicals such as H, OH and O. They analyzed their data using a classical kinetic approach. However, they did not perform a detailed computer modeling of their experiments. Such study could give new and needed information about the combustion chemistry of methanol and especially CH_2OH and CH_3O reactions.

Table 1 lists the three Vandooren and Van Tiggelen well-studied burner-stabilised laminar premixed flames compositions and operating conditions that the developed model has been compared against. As a first step, the discussion will be focused on the ability of the model to correctly predict the mole fraction profiles of the reactants, intermediates and products in the three flames.

Vandooren and Van Tiggelen data as well as the numerical calculations are showed in Figs. 1a–1d and Table 2. From these results it can be seen that, in the

Table 1. Initial conditions of laminar flames of lean premixed $CH_3OH/O_2/Ar$ (flame I), CH_3OH/O_2 (flame II) and $CH_3OH/H_2/O_2$ (flame III)

Flame	Flame characteristics						
	concentration, %				equivalence ratio	pressure, Torr	initial velocity of the fresh gases, cm/s
	$[CH_3OH]$	$[O_2]$	[Ar]	$[H_2]$			
I	19.9	33.7	46.4	–	0.89	40	43
II	19.4	80.6	–	–	0.36	40	40
III	10.9	85.9	–	3.2	0.21	40	78

Table 2. Mole fractions and positions of the maxima of the various species measured in the three flames of Vandooren and Van Tiggelen [7] at $T_0 = 298$ K and $P = 0.0526$ atm

Specie	Flame	Max mole fraction					Max position, cm				
		experiment	our model	XD	Egolfopolous	Pauwels	experiment	our model	XD	Egolfopolous	Pauwels
H	I	0.012	0.009	0.008	0.001	0.012	0.719	0.662	0.584	0.861	0.903
	II	0.004	0.008	0.005	0.005	0.007	0.706	0.699	1.125	1.105	1.1391
	III	0.009	0.004	0.004	0.004	0.006	1.003	0.998	1.361	1.244	1.203
H_2	I	0.038	0.026	0.019	0.017	0.030	0.194	0.078	0.078	0.070	0.096
	II	0.009	0.008	0.004	0.004	0.007	0.250	0.167	0.200	0.171	0.214
	III	0.025	0.022	0.022	0.021	0.022	0.053	0.047	0.047	0.053	0.047
O	I	0.009	0.007	0.006	0.008	0.006	0.717	0.682	0.510	1.486	0.902
	II	0.014	0.014	0.017	0.018	0.013	0.590	0.665	1.070	0.864	1.132
	III	0.021	0.020	0.023	0.023	0.018	0.469	0.903	1.349	1.266	1.212
OH	I	0.022	0.020	0.019	0.021	0.017	0.722	1.173	1.179	1.297	1.284
	II	0.024	0.023	0.025	0.025	0.020	0.650	0.644	0.919	0.812	0.845
	III	0.019	0.023	0.026	0.026	0.022	0.412	0.848	1.292	1.252	1.218
CO	I	0.100	0.081	0.083	0.083	0.088	0.222	0.157	0.150	0.150	0.179
	II	0.063	0.066	0.073	0.071	0.070	0.251	0.222	0.287	0.222	0.287
	III	0.062	0.052	0.058	0.056	0.054	0.380	0.409	0.480	0.452	0.480
CH_2O	I	0.012	0.011	0.006	0.005	0.010	0.133	0.062	0.035	0.047	0.047
	II	0.008	0.009	0.0083	0.006	0.009	0.197	0.173	0.176	0.129	0.164
	III	0.009	0.008	0.007	0.005	0.007	0.311	0.320	0.365	0.347	0.362
CH_3O	I	9.00×10^{-5}	1.16×10^{-4}	3.68×10^{-4}	9.85×10^{-5}	2.50×10^{-3}	0.219	0.168	0.016	0.082	0.096
	II	3.42×10^{-5}	5.49×10^{-5}	1.15×10^{-4}	2.0×10^{-4}	8.98×10^{-3}	0.252	0.216	0.252	0.027	0.252
	III	3.05×10^{-5}	8.03×10^{-5}	1.16×10^{-4}	8.96×10^{-5}	6.65×10^{-4}	0.338	0.358	0.248	0.293	0.410

case of flame I, Pauwels model overpredicts the O_2 mole fraction, especially for the high distances from the burner, whereas a good accuracy was obtained between the computed, using the three other models, and the experimental O_2 mole fraction profiles. In the case of flames II and III, all the used models underpredict the O_2 mole fraction profile, especially near the burner surface (Fig. 1a). This effect may be ascribed to the flame disturbance by the MBMS sampling cone. Concerning methanol, it is obvious that for flames I and II, except for Pauwels model which matches well the experimental data, the CH_3OH profiles computed with the three other models start slightly before the corresponding experimental profiles, but for flame III these computed profiles are slightly delayed compared with the experimental profiles, except for our model which gives a good accordance between calculated and measured data (Fig. 1b). For the stable combustion products, the used models predict well the experimental data in the reaction zone; however the rates of CO_2 and H_2O formation are somewhat slower than the experimental values at the end of the reaction (Figs. 1c

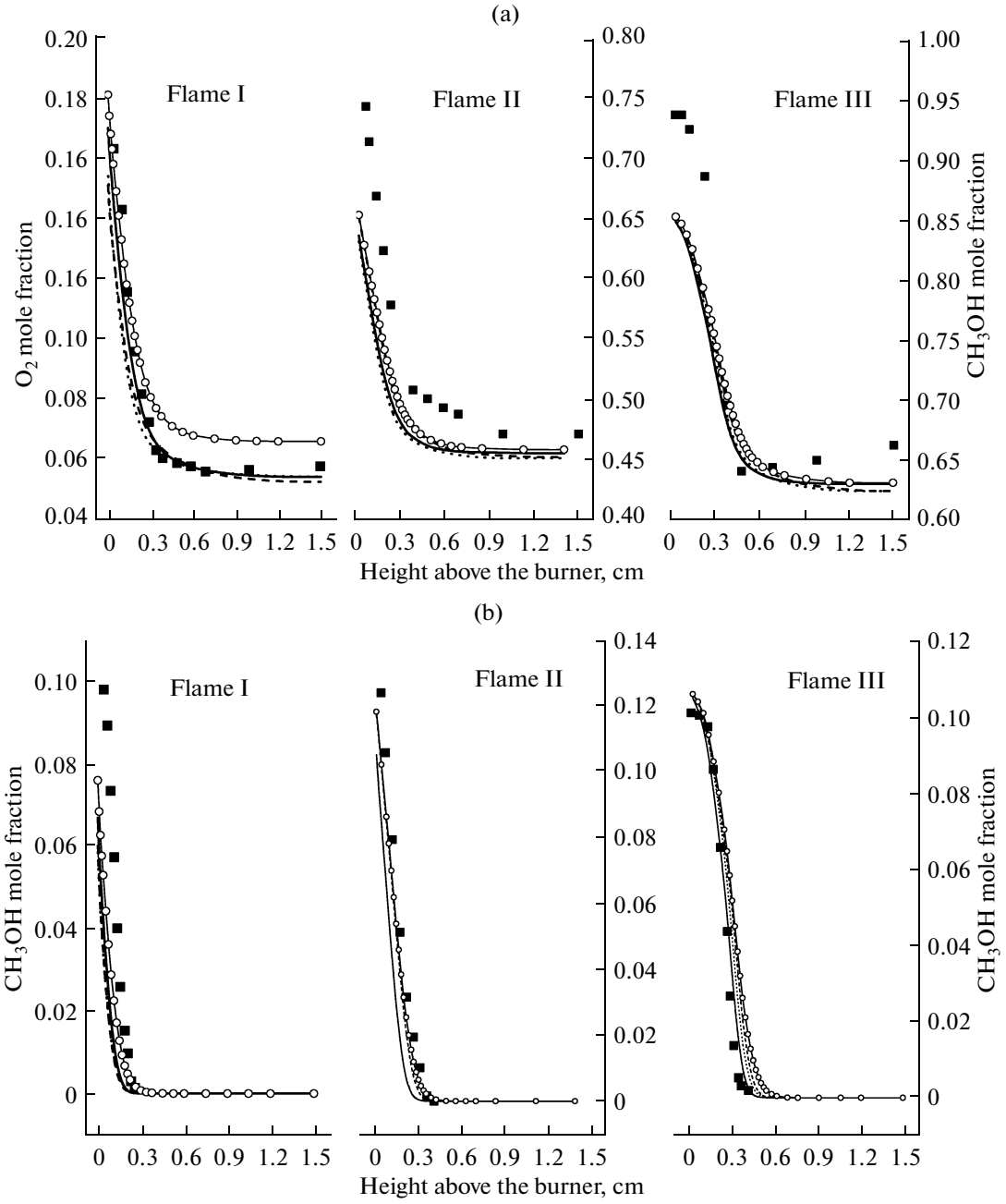

Fig. 1. Comparison between computed (lines) and experimental (Vandooren and Van Tiggelen [7], symbols ■—mole fraction profiles of O_2 (a), CH_3OH (b), CO_2 (c) and H_2O (d) for the three flames at $T_0 = 298$ K and $P = 0.0526$ atm: — our model, - - - HD model, ···· Egolfopolous model, —○— Pauwels model.

and 1d). By comparison to the other models, our proposed model is somewhat better than the other in predicting both the initial and the final concentrations of CO_2 especially in the case of flames II and III.

The models behaviors in predicting H mole fraction profiles are dependent on the flame composition, Pauwels model is the best in the case of flame I whereas it is the worst in the case of flames II and III. Opposite trends are observed for our proposed model (Table 2). Besides, a good ability in reproducing the H_2 profiles shape (mole fraction and position of the maximum) is shown by the proposed model for the three flames, while the other models fail to reproduce these shapes in the case of flames I and II (Table 2). In addition, it can be observed from these results that the proposed model predicts both the shape (position) and the value of O and OH mole fraction profiles with a good accuracy as compared to the other mechanisms. Furthermore, it can be seen that all the used models predict well the CO mole fraction profiles, except for the Pau-

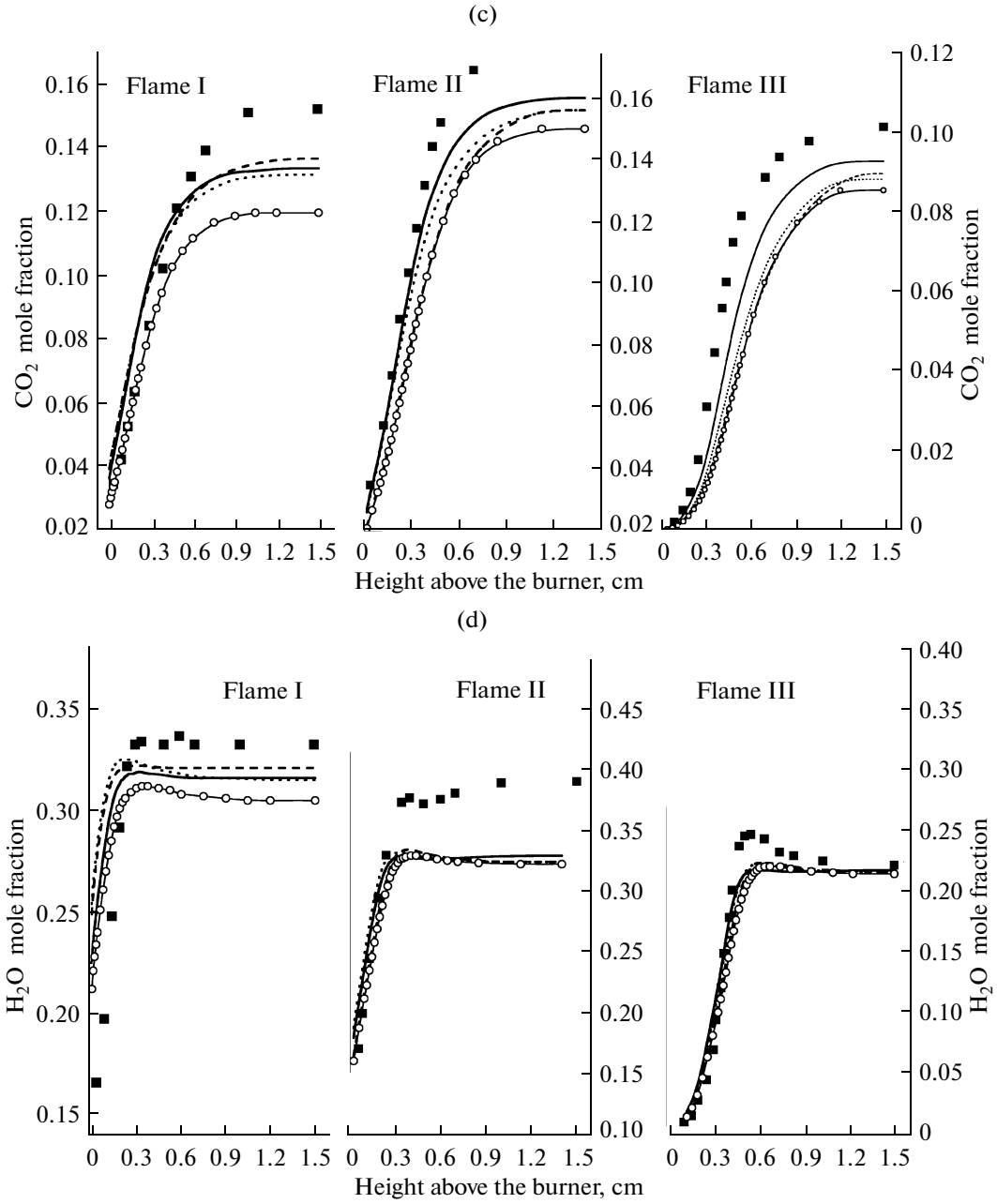

Fig. 1. Contd.

wels model which gives higher values as compared to the experience, especially at the end of the reaction (figure not shown).

As mentioned in the open literature, the relative amount of formaldehyde (CH_2O) present as an intermediate species is important, particularly due to concerns over its presence as a toxic emission product in methanol-fueled vehicles [25, 36]. It was reported that formaldehyde has adverse effects on the environment due to its smell and that it may have carcinogenic effects. Furthermore, it was observed that once emitted, the lifetime of formaldehyde in the atmosphere is considerable, of the order of hours or even days. It is a very active compound in the tropospheric chemistry, participating in chain-propagating reactions through photolysis and by interaction with OH radicals, thereby contributing to photochemical smog [37]. These observations suggest that the ability of a model to reproduce the formaldehyde quantity has a great importance in the validation of this model. Table 2 shows the comparisons between calculations using the four schemes and the experimental data for flames I, II, and III as reported by Vandooren and Van Tiggelen at $P = 0.053$ atm (40 Torr) [7]. It is seen that the calcu-

Table 3. Mole fractions and positions of the maxima of the various species measured in Pauwels' flame [20] at P = 0.105 atm and $\Phi = 1.08$

Specie	Max mole fraction					Max position, cm				
	experiment	our model	XD	Egolfopolous	Pauwels	experiment	our model	XD	Egolfopolous	Pauwels
H	0.004	0.003	0.009	0.008	0.011	0.536	0.567	0.777	0.834	0.883
H_2	0.014	0.021	0.019	0.017	0.028	0.252	0.252	0.143	0.139	0.209
O	0.002	0.001	0.002	0.002	0.002	0.351	0.494	0.524	0.502	0.615
OH	0.003	0.003	0.005	0.005	0.004	0.681	0.614	0.598	0.568	0.605
CO	0.046	0.059	0.061	0.059	0.062	0.255	0.347	0.198	0.169	0.261

lated values, in the case of flames I and III, are somewhat lower than the measured ones, with the proposed model giving the best accuracy. For flame I, the computed CH_2O concentration, using our model, is lower than the experimental one by a factor of 1.07, whereas the concentrations computed, using the models HD, Egolfopolous and Pauwels, are lower by a factor of 1.9, 2.72 and 1.18, respectively. For flame III, the calculated CH_2O mole fraction, using the proposed model, is lower than the experimental one by a factor of 1.17, whereas the mole fractions calculated, using the models HD, Egolfopolous and Pauwels, are lower by a factor of 1.37, 1.78 and 1.29, respectively. In the case of flame II, the computed CH_2O concentrations for the proposed model, HD and Pauwels models are larger than the experimental ones by a factor of 1.31, 1.07 and 1.16, respectively, whereas Egolfopolous underpredicts the CH_3O concentration by a factor of 1.34.

Concerning CH_3O (a combination of methoxy CH_2OH and hydroxymethyl radicals CH_2OH), which is one of the most important intermediate in the methanol oxidation, the collected data suggest that for flame I, a relative spatial shift and a very good concentrations values are observed for the computed data using our model, whereas a relative spatial shift and a lower concentration, by a factor of 1.2 are observed on the computed concentration using Egolfopolous model. On the other hand, HD and Pauwels models overpredict the CH_2O concentration by a factor of 3.24 and 21.85, respectively. In the case of flame II, our model matches well the experimental data, whereas HD, Egolfopolous and Pauwels models overpredict the CH_3O concentrations by a factor of 2.48, 4.33 and 18.58, respectively. Besides, it is noteworthy that the profile shape obtained when using Egolfopolous model is different from the experimental one (Figure not shown). In the case of flame III, the shape of the calculated CH_3O mole fraction and the position of its maximum, using our model, match well the experimental ones, whereas the peak value seemed to be overpredicted (a factor of 1.44 is observed). Besides, the CH_3O profile computed with HD model start slightly before the corresponding experimental profile and the magnitude of the predicted data are higher than the experimental ones by a factor of 2.12, while this computed profile is slightly delayed compared with the experimental profile and the value of the maximum mole fraction is higher by a factor of 11.60 in the case of the calculated data using Pauwels model. Finally, it is noteworthy that the CH_3O mole fraction profile shape obtained by Egolfopolous model (two maxima) is different from the experimental one.

Validation on Stoichiometric Flames

Pauwels et al. [20] reported the structure of a stoichiometric methanol-air flame stabilised in a horizontal low pressure flat flame burner. The flow velocity was 26.4 cm/s at 0.105 atm. Sampling was performed with a quartz probe and the concentrations were determined by using electron spin resonance spectroscopy for paramagnetic species as H, O, and OH, and gas chromatography for the stable species. The temperature was measured with a 50 μm diameter Pt–Rh thermocouple coated with a thin layer of beryllium and yttrium oxides to reduce catalytic effects.

Figures 2a and 2b as well as Table 3 compare calculations using the four models and the experimental data as reported by Pauwels and coworkers [20]. In the case of molecular oxygen, the predicted mole fraction profiles by Pauwels model match well the measured ones until a distance from the burner of 0.45 cm. Above this distance, the model overpredicts the O_2 concentration (Fig. 2a). Using our model, the O_2 concentration is predicted closely within the fuel consumption zone, except for the range 0.33–0.65 cm where the calculated values are somewhat higher than the measured ones. Besides, for the low distances from the burner, the O_2 profiles computed with HD and Egolfopolous models start slightly before the corresponding experimental profiles, whereas for the high distances from the burner, a good accuracy was obtained between the computed and the experimental O_2 mole fraction profiles. On the other hand, the CH_3OH concentration is predicted closely within the fuel consumption zone when using Pauwels or our proposed model, and it starts slightly before the corre-

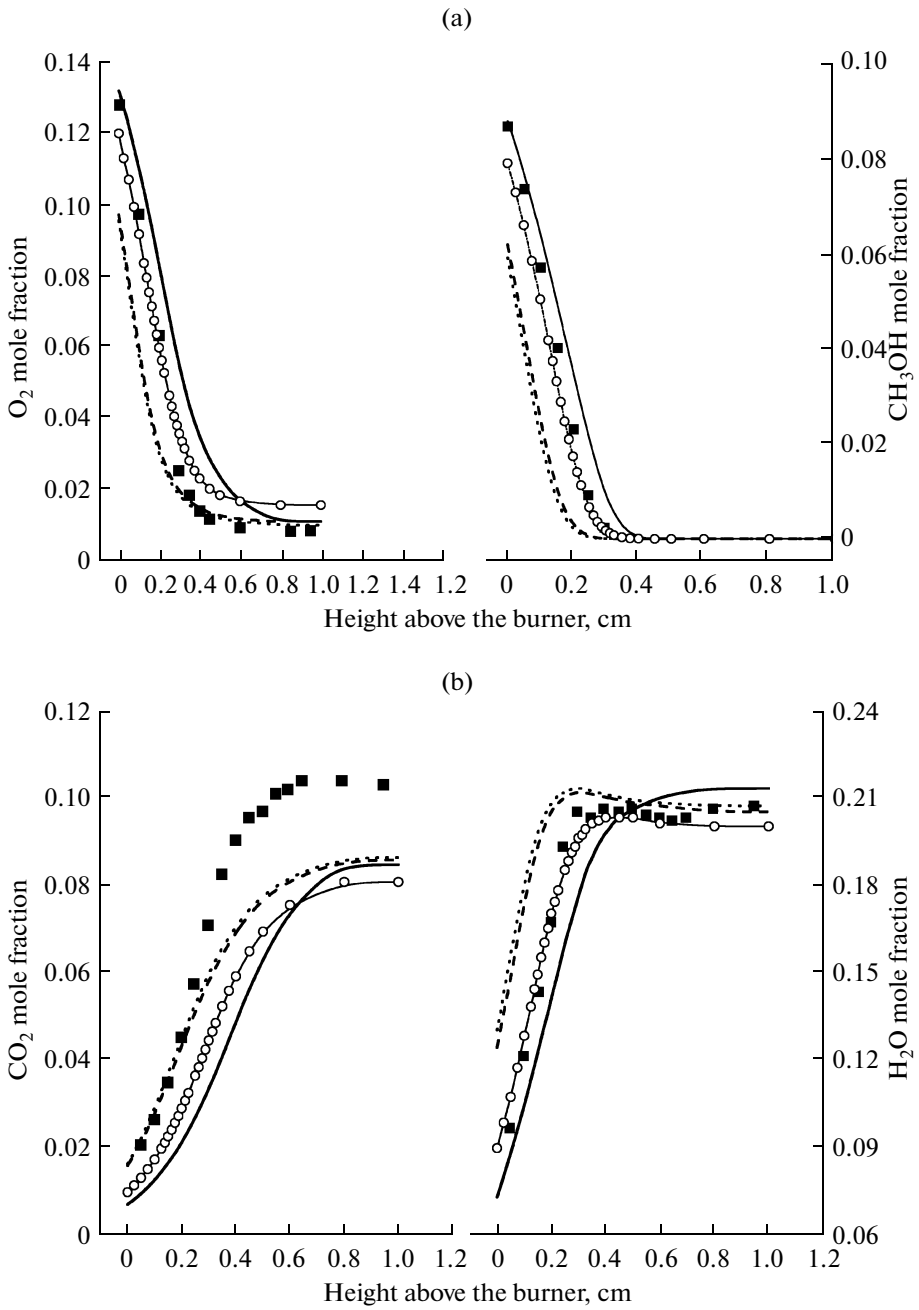

Fig. 2. Comparison between computed (lines) and experimental (Pawels experience [20], symbols ■) mole fraction profiles of O_2 and CH_3O (a), CO_2 and H_2O (b) at $P = 0.105$ atm and $\Phi = 1.08$: — our model, - - - HD model, ···· Egolfopolous model, —○— Pauwels model.

sponding experimental profiles when using HD or Egolfopolous model (Fig. 2a).

For the stable combustion products, the used models predict well the experimental data for H_2O, whereas the rates of CO_2 formation are somewhat slower than the experimental values especially at the end of the reaction (Fig. 2b).

From the results consigned in Table 3, it can clearly be seen that the proposed model exhibits a good ability in reproducing both profile shape (position of the maximum) and H concentration values, whereas the models HD, Egolfopolous and Pauwels overpredict the H mole fraction by a factor of 2.65, 2.47 and 3.29, respectively. Besides, the H_2 mole fraction is overpredicted by a factor of 1.97, 1.52, 1.31 and 1.22 for Pauwels, the proposed, HD and Egolfopolous models, respectively. In addition, the proposed model displays a good ability in reproducing the position of the O maximum. However it overpredicts its concentration value by a factor of 1.65, whereas the other used mod-

els fail to reproduce the shape of O mole fraction profiles (maximum position). Moreover, they overpredict the O concentration values by a factor of 1.71, 1.65 and 1.53 for HD, for Pauwels and Egolfopolous models, respectively. On the other hand, the proposed model predicts both the shape and the value of OH mole fraction profiles with a good accuracy, whereas the HD, Egolfopolous and Pauwels models overpredict this radical species concentrations values by a factor of 1.50, 1.43 and 1.38, respectively. Finally, it is noteworthy that the four models exhibit a good ability to reproduce the CO mole fraction profiles shape; however the calculated concentration values are somewhat higher than the measured ones.

Validation on Rich Flames

Bradley et al. [33] measured the structure of a moderately rich laminar, flat, adiabatic methanol-air flame on a matrix burner of 76 mm diameter. Gas temperatures were measured by a silica coated Pt-20%Rh—Pt-40%Rh thermocouples, formed from wires of 50 μm diameter while a microprobe was used for species sampling and gas chromatography for species analysis.

Figures 3a–3c show the comparisons between calculations using the four schemes and the experimental data as reported by Bradley and coworkers at a pressure of 0.089 atm and an equivalence ratio $\Phi = 1.25$. From these figures, it can be seen that the studied models predict with a good accuracy the O_2 mole fraction profile, whereas the computed CH_3OH profiles are slightly delayed as compared to the experimental data (Fig. 3a). On the other hand, it is obvious that the four schemes show a good ability in reproducing the CO_2 profiles shape, whereas they underpredict its concentration values by a factor of 1.04, 1.10, 1.16 and 1.18 for the proposed model, Egolfopolous, HD and Pauwels model, respectively. Same trends are observed in the case of CO (Fig. 3b). As in the case of CO_2 and CO, the H_2 mole fraction profile shape is well predicted by the four models, whereas its concentration values are somewhat overpredicted (Fig. 3c).

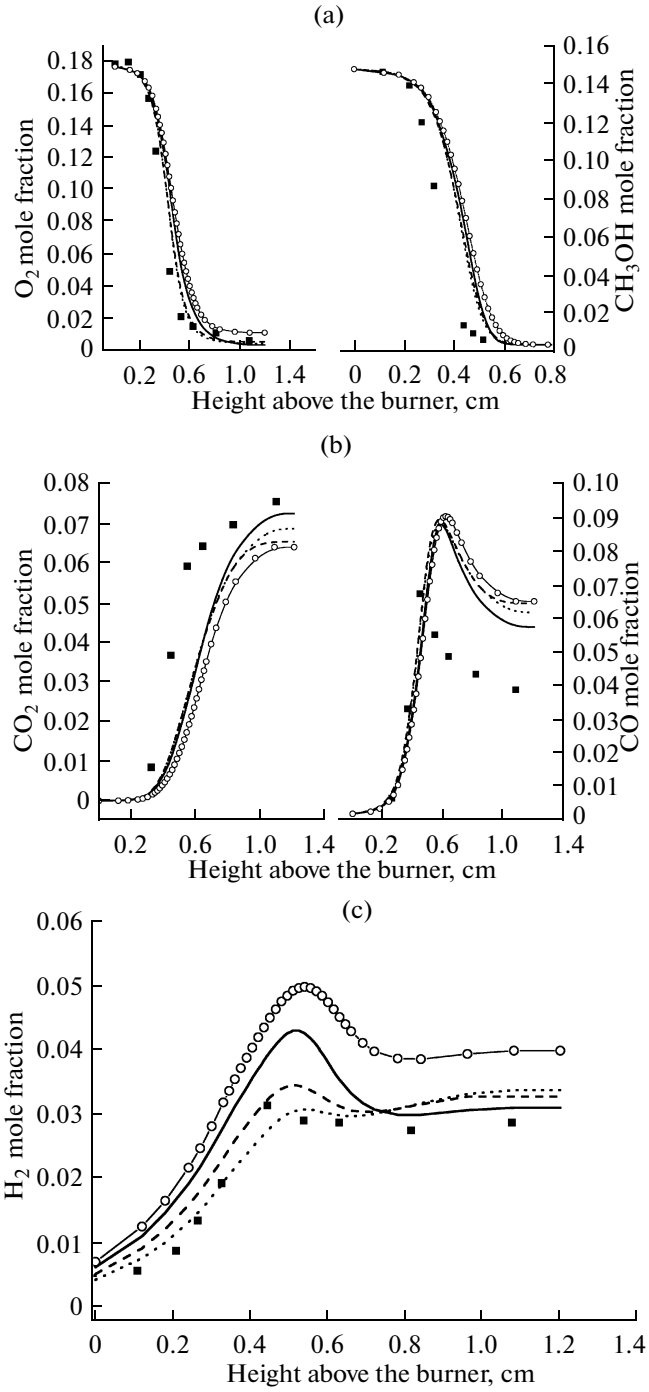

Fig. 3. Comparison between computed (lines) and experimental (Bradley experience [33], symbols ■) mole fraction profiles of O_2 and CH_3OH (a), CO_2 and CO (b), H_2 (c) at $P = 0.089$ atm and $\Phi = 1.25$: — our model, - - - HD model, ···· Egolfopolous model, –○– Pauwels model.

KINETIC ANALYSIS

Production and consumption rates were the main criteria in the kinetic analysis. The appropriate subroutines in the Chemkin package (CKQYP, CKCON) [27] were used to systematically compute the rate of production and/or consumption of each species.

Following the Chemkin formalism, for each species k, the production rate k(w_k) can be written as a summation of the rate of progress variables for all reactions (K) involving the kth species, where the rate of progress variable q_i for the ith reaction is given by the difference of the forward and reverse rates as:

$$q_i = k_{fi}\prod_{k=1}^{K}[X_k]^{\nu'_{ki}} - k_{ri}\prod_{k=1}^{K}[X_k]^{\nu''_{ki}},$$

where X_k is the molar concentration of the kth species and k_{fi} and k_{ri} are the forward and reverse rate con-

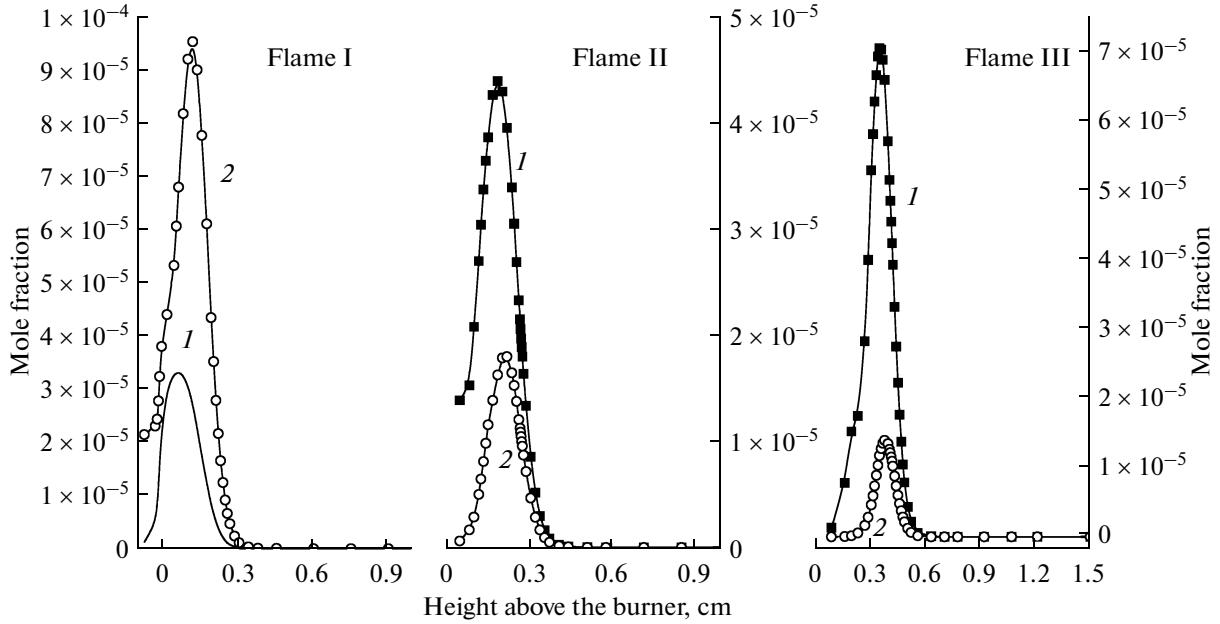

Fig. 4. Computed CH_3O (*1*) and CH_2OH (*2*) mole fractions for the three flames of Vandooren and Van Tiggelen.

stants of the *i*th reaction. Following El-Bakali et al. procedure [38], the involved reactions, for species k, are sorted out in respect to their maximum absolute rate. Their sign indicated the species consumption or formation. Then they are rearranged to determine the species flux when the same species are involved in both hands. It is well known that the rate of progress is dependent on the species concentration and the temperature as well; these two entities are dependent on the location. So, in the aim to take this variation along the burner axis into account, integration of the rate of progress versus the height above the burner was chosen to consider the species molar flux. The integrated rate of progress for each reaction or group of reactions represents the contribution of this reaction or group of reactions to the species formation or consumption (according to the sign of the rate of progress). In order to describe the methanol oxidation pathways, the individual contributions of the elementary reactions to the global evolution rates for each species were calculated and the main reactions relative to specified species analyzed were delineated. In this section, only the main reactions which have an important role in chemicals belonging system C_1 (CH_3OH, CH_2OH, CH_3O, CH_2O) will be presented (Figs. 4 and 5 and Table 5). H_2/O_2 and CO/CO_2 systems are relatively well known. Reaction mechanism in methanol is presented in the Table 4.

Kinetic Analysis in Lean Flames

Fuel (CH_3OH) destruction. After the initial decomposition of methanol, the major paths consuming fuel, in the three flames of Vandooren and Van Tiggelen [7], is the H, O and OH attack leading to H abstraction, according to (the numbers in parenthesis correspond to numbers of reaction in the Table 4):

(86) $CH_3OH + OH = CH_3O + H_2O$,

(87) $CH_3OH + O = CH_2OH + OH$,

(89) $CH_3OH + OH = CH_2OH + H_2O$,

(90) $CH_3OH + H = CH_2OH + H_2$,

(103) $CH_3OH + O = CH_3O + OH$.

The contribution of each reaction in the methanol consumption is dependent on the flame composition. Reactions 86 and 87 contribute with 18.01, 27.37, 27.30 and 5.25, 10.61, 12.73% for flames I, II and III, respectively. The contribution of reactions 89 and 90 are evaluated to 20.75, 29.15, 28.83 and 50.35, 23.08, 19.25% for flames I, II and III, respectively. Finally, the reaction 103 accounts for 4.27, 9.15 and 11.35% to the total CH3OH decomposition for flames I, II and III, respectively. These findings suggest that the reaction between CH_3OH and OH is the main consumption step for methanol and that the abstraction may occur at either the methyl or hydroxyl group, forming $CH_2OH + H_2O$ (89) or $CH_3O + H_2O$ (86), respectively. Measurements of the overall rate constant range from low temperature [77–82] to a temperature of 2000 K [7, 73, 83–87]. In general, the scatter increases with temperature and the high-temperature studies mostly involve indirect measurements [14]. As mentioned by Held and Dryer [23], overall rates for the reaction of methanol with OH were reported by two recent studies. An expression for $k_{89} + k_{86} = 3.54 \times 10^4 T^{2.6}\exp(883/RT)$ over the temperature range 293–803 K was obtained by Hess and Tully [87] who estimated the "branching ratio", defined as $k_{89}/(k_{89} + k_{86})$, using isotopic substitution. This branching ratio increased from a small value to 0.5 at their highest

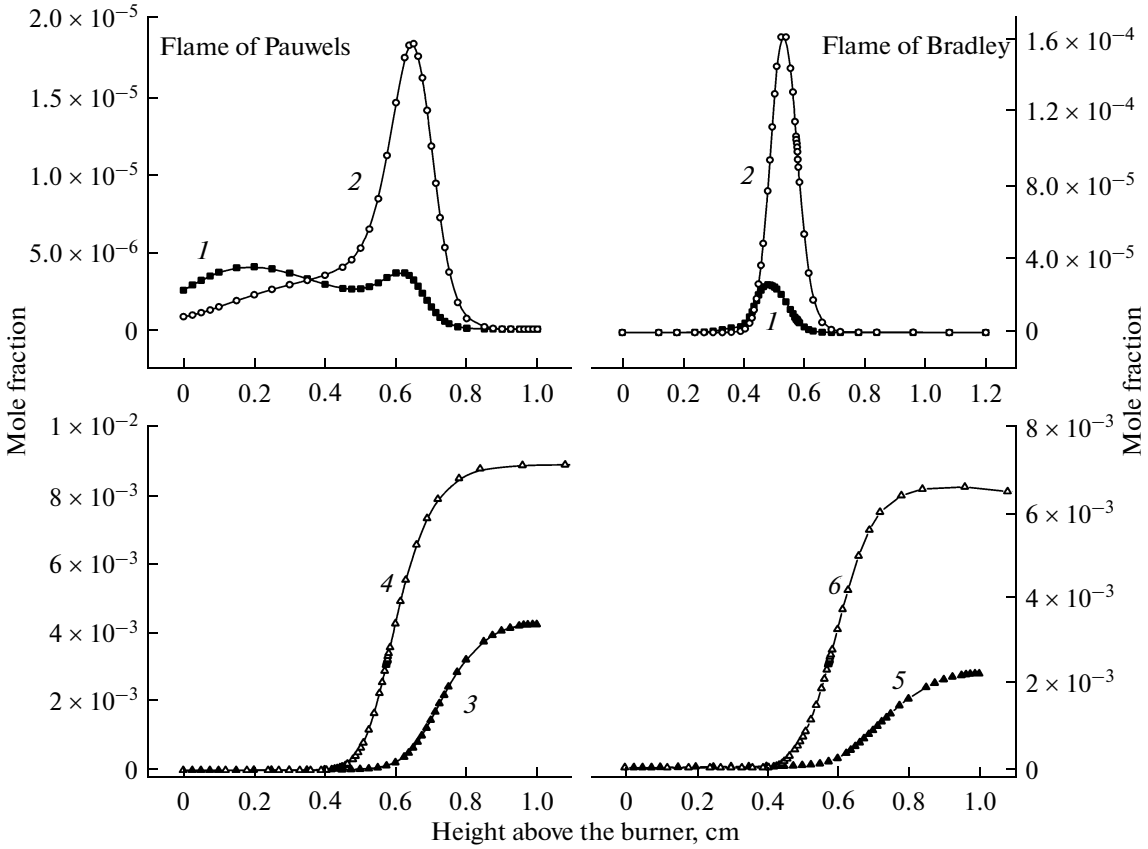

Fig. 5. Computed mole fractions CH_3O (*1*), CH_2OH (*2*), H in flames of Pauwels (*3*) and Bradley (*4*), and OH in flames of Pauwels (*5*) and Bradley (*6*).

temperature. More recently, a value for $k_{89} + k_{86}$ of 5.2×10^{12} mol cm^{-3} s^{-1} at 1200 K was obtained by Bott and Cohen [73], in excellent agreement with the value of 5.1×10^{12} obtained from the previous expression. Their calculated site specific expressions yield a branching ratio that increases from 0.39 at 1000 K to 0.51 at 2000 K. In this study the branching ratio vary from 0.48 to 0.58 in the temperature range 1000–2000 K.

In all cases, it is obvious that CH_3OH consumption produces only hydroxymethyl (CH_2OH) and methoxy (CH_3O) radicals. As mentioned in the open literature, despite the extensive past efforts, important aspects of methanol chemistry are still unresolved. One important issue concerns the relative importance of the two fuel-derived radicals, hydroxymethyl (CH_2OH) and methoxy (CH_3O) [14]. Thus we have computed the two radicals' mole fraction, using our model, for the three flames of Vandooren and Van Tiggelen and the results are depicted in Fig. 4. It is clearly seen that the relative importance of the two isomers is dependent on the flame composition. For flame I, the maximum of CH_3OH concentration is larger than that of CH_3O by a factor of 2.86. This fact may be ascribed to the fact that, in the case of flame I, CH_2OH is mainly consumed (76.53%) via channels forming the radical hydroxymethyl (reactions 90, 89 and 87) which is in agreement with the fact that bond energies in methanol favour CH_2OH formation. The opposite trend was observed for flames II and III, where the maximum concentration of CH_3O is larger than that of CH_2OH by a factor of 2.45 and 5.05 for flame II and flame III, respectively. Although in the latter two flames, methanol oxidation leads mainly to CH_2OH, the observed concentration of this latter is lower than the one of CH_3O which means that in these flames CH_2OH is more reactive than CH_3O.

Reactions of CH_2OH/CH_3O and CH_2O radicals. The most important intermediates from initial methanol oxidation are methoxy CH_2OH and hydroxymethyl CH_3O radicals. These intermediates were found to be a very important species in the higher hydrocarbon oxygenates oxidation and pyrolysis [36]. Since these two isomers tend to travel different paths, it is very important to distinguish between them.

a—CH_2OH reactions

As above mentioned, the CH_2OHradical is formed from methanol via the reactions 87, 89 and 90:

(87) $CH_3OH + O = CH_2OH + OH$,

(89) $CH_3OH + OH = CH_2OH + H_2O$,

(90) $CH_3OH + H = CH_2OH + H_2$.

Table 4. Methanol oxidation reaction mechanism*

No.	Reaction**	A	n	E	Reference
1	$H + O_2 = OH + O$	1.900×10^{14}	0.0	16812.0	39
2	$H + H + M = H_2 + M$ $Ar/0.63/CH_4/2.00/$	1×10^{18}	−1.0	0.0	35
3	$O + O + M = O_2 + M$ $H_2O/15.4/CO/1.75/CO_2/3.6/CH_4/2.0/H_2/2.4/Ar/0.84/$	1.20×10^{17}	−1.0	0.0	57
4	$H_2 + O_2 = OH + OH$	1.700×10^{13}	0.0	47780.0	58
5	$O + H_2 = OH + H$	3.870×10^{4}	2.7	6260.0	45
6	$H + O_2 + M = HO_2 + M$ $CO/0.75/\ CO_2/1.5/$	2.800×10^{18}	−0.9	0.0	59
7	$H + OH + M = H_2O + M$ $H_2O/3.65/CH_4/2.0/H_2/0.73/Ar/0.38/$	2.20×10^{22}	−2.0	0.0	41
8	$H_2 + OH = H_2O + H$	2.161×10^{8}	1.51	3430.0	60
9	$OH + OH = O + H_2O$	3.570×10^{4}	2.4	−2110	56
10	$HO_2 + H = O_2 + H_2$	1.660×10^{13}	0.0	820	44
11	$HO_2 + H = OH + OH$	7.080×10^{13}	0.0	300	44
12	$H + HO_2 = H_2O + O$	3.010×10^{13}	0.0	1721.0	39
13	$H + H + H_2 = H_2 + H_2$	9.00×10^{16}	−0.6	0.0	41
14	$H + H + H_2O = H_2 + H_2O$	6.00×10^{19}	−1.3	0.0	41
15	$H + H + CO_2 = H_2 + CO_2$	5.50×10^{20}	−2.0	0.0	41
16	$H + O_2 + O_2 = HO_2 + O_2$	3.00×10^{20}	−1.7	0.0	41
17	$H + O_2 + H_2O = HO_2 + H_2O$	1.65×10^{19}	−0.8	0.0	41
18	$H + O_2 + Ar = HO_2 + Ar$	7.00×10^{17}	−0.8	0.0	41
19	$O + OH + M = HO_2 + M$	1.00×10^{17}	0.0	0.0	62
20	$OH + OH(+M) = H_2O_2(+M)$ Low/0.22110¥10^{20} −0.76 0.0 TROE/0.50 0.10¥10^{9} 0.10¥10^{-5}/ $H_2O/16.25/CO/1.875/CO_2/3.75/CH_4/16.25/H_2/2.5/$	7.22×10^{13}	−0.4	0.0	40
21	$C + O_2 = CO + O$	2.00×10^{13}	0.0	0.0	63
22	$HO_2 + OH = H_2O + O_2$	2.890×10^{13}	0.0	−497.0	40
23	$HO_2 + O = OH + O_2$	1.810×10^{13}	0.0	−397.0	41
24	$HO_2 + HO_2 = H_2O_2 + O_2$ (Deplicate)	4.20×10^{14}	0.0	11982.0	47
25	$HO_2 + HO_2 = H_2O_2 + O_2$ (Deplicate)	1.30×10^{11}	0.0	−1630.0	47
26	$H_2O_2 + OH = HO_2 + H_2O$ (Deplicate)	5.800×10^{14}	0.0	9557.0	65
27	$H_2O_2 + OH = HO_2 + H_2O$ (Deplicate)	1.750×10^{12}	0.0	320	43
28	$H_2O_2 + H = HO_2 + H_2$	1.700×10^{12}	0.0	3750.0	39
29	$H_2O_2 + H = HO_2 + H_2$	1.700×10^{12}	0.0	3750.0	39
30	$H_2O_2 + H = H_2O + OH$	1.017×10^{13}	0.0	3590.0	39
31	$H_2O_2 + O = OH + HO_2$	9.630×10^{6}	2.0	4000	43
32	$H_2O_2 + O = O_2 + H_2O$	9.55×10^{6}	2.0	3970.0	50
33	$C + OH = CO + H$	5.00×10^{13}	0.0	0.0	60
34	$CO + HO_2 = CO_2 + OH$	3.010×10^{13}	0.0	23000.0	54
35	$CO + OH = CO_2 + H$	4.760×10^{7}	1.228	70	43
36	$CO + O(+M) = CO_2(+M)$ Low/1.55E^{24} 22.79 4190/ $H_2O/12.0/CO/1.9/CO_2/3.8/H_2/2.5/Ar/0.87/$	1.8×10^{10}	0.0	2380	48
37	$CO + O_2 = CO_2 + O$	2.529×10^{12}	0.0	47846.88	41
38	$HCO + M = H + CO + M$ $CO/1.9/CO_2/3.8/H_2O/6.0/H_2/2.5/$	4.75×10^{11}	0.7	14900.0	24
39	$HCO + OH = CO + H_2O$	1.000×10^{14}	0.0	0.0	39
40	$HCO + O = CO + OH$	3.000×10^{13}	0.0	0.0	39
41	$HCO + O = CO_2 + H$	3.000×10^{13}	0.0	0.0	39
42	$HCO + H = CO + H_2$	7.224×10^{13}	0.0	0.0	46
43	$HCO + O_2 = CO + HO_2$	1.35×10^{13}	0.0	400.0	61
44	$HCO + CH_3 = CO + CH_4$	1.200×10^{14}	0.0	0.0	41
45	$HCO + HO_2 = CO_2 + OH + H$	3.000×10^{13}	0.0	0.0	41

Table 4. (Contd.)

No.	Reaction**	A	n	E	Reference
46	$HCO + HCO = CH_2O + CO$	3.0×10^{13}	0.0	0.0	49
47	$HCO + HCO = H_2 + CO + CO$	3.000×10^{12}	0.0	0.0	41
48	$CH_4 + O = CH_3 + OH$	1.620×10^{6}	2.30	7094.0	67
49	$CH_4(+M) = CH_3 + H(+M)$ Low/0.4515 ¥ 10^{18} 0.00 ¥ 10^{0} 0.90815 ¥ 10^{5}/ TROE/0.640 ¥ 10^{0} 0.100 ¥ 10^{-14} 0.3195 ¥ 10^{4} 0.12126 ¥ 10^{5}/	2.40×10^{16}	0.0	104920.0	70
50	$CH_4 = CH_3 + H$	4.5232×10^{17}	0.0	90909.09	40
51	$CH_4 + HO_2 = CH_3 + H_2O_2$	1.81×10^{11}	0.0	18600.0	41
52	$CH_4 + H = CH_3 + H_2$	5.47×10^{7}	2.00	11200	51
53	$CH_3 + HO_2 = CH_4 + O_2$	3.16×10^{12}	0.0	0.0	52
54	$CH_3 + OH(+M) = CH_3O + H(+M)$ Low/1.713 ¥10^{18} −0.02 13083.0/ H_2O/16.0/CO2/3.75/CO/1.875/H_2/2.5/CH_4/16.0/	9.95×10^{14}	−0.82	16872.0	71
55	$CH_3 + OH(+M) = CH_2O + H_2(+M)$ Low/7.801 ¥ 10^{16} −0.03 8786.0/ H_2O/16.0/CO_2/3.75/CO/ 1.875/H_2/2.5/CH_4/16.0/	7.39×10^{14}	−1.13	14551.0	71
56	$CH_3 + OH = HCOH + H_2$	1.00×10^{10}	0.0	−415.0	72
57	$CH_3 + O_2 = CH_3O_2$	9.03×10^{58}	−15.0	17023.0	41
58	$CH_3 + O = HCO + H_2$	1.26×10^{13}	0.0	0.0	75
59	$CH_3 + O = CH_3O$	1.78×10^{14}	−2.1	603.0	68
60	$CH_3 + HO_2 = CH_3O + OH$	2.41×10^{10}	0.80	−2330	53
61	$CH_3 + OH = CH_2OH + H$	1.99×10^{19}	−1.7	11157.0	71
62	$CH_3 + OH = CH_2O + H_2$	4.170×10^{10}	−0.03	8786.0	71
63	$CH_3O + H = CH_3 + OH$	3.20×10^{13}	0.0	0.0	55
64	$CH_3 + O = CH_2O + H$	8.4322×10^{13}	0.0	0.0	39
65	$CH_3 + O_2 = O + CH_3O$	1.99×10^{18}	−1.60	29200	41
66	$CH_3 + CH_3O = CH_4 + CH_2O$	2.409×10^{13}	0.0	0.0	41
67	$CH_3 + CH_2OH = CH_4 + CH_2O$	2.410×10^{12}	0.0	0.0	42
68	$CH_3O + H = CH_2OH + H$	3.40×10^{6}	1.6	0.0	43
69	$CH_3O + H(+M) = CH_3OH(+M)$ Low/8.600 ¥ 10^{28} −4 3025/ TROE/0.8902 144.000 2838.0 45569.0/ CO/1.5/CO_2/2.0/H_2O/6.0/H_2/2.0/CH_4/2.0/	5.000×10^{13}	0.0	0.0	43
70	$CH_3O + M = CH_2O + H + M$ H_2O/5.00/	8.30×10^{17}	−1.2	15500.0	74
71	$CH_3O + HO_2 = CH_2O + H_2O_2$	3.011×10^{11}	0.0	0.0	41
72	$CH_3O + O = CH_2O + OH$	6.000×10^{12}	0.0	0.0	41
73	$CH_3O + H = CH_2O + H_2$	1.987×10^{13}	0.0	0.0	41
74	$CH_3O + O_2 = CH_2O + HO_2$	2.168×10^{10}	0.0	1751.1	40
75	$CH_3O + CH_2O = CH_3OH + HCO$	1.017×10^{11}	0.0	2983.2	41
76	$CH_3O + CO = CH_3 + CO_2$	1.572×10^{13}	0.0	11814.7	41
77	$CH_3O + HCO = CH_3OH + CO$	9.034×10^{13}	0.0	0.0	41
78	$CH_2O + M = HCO + H + M$ H_2O/16.25/CO/1.875/CO_2/3.75/CH_4/16.25/H_2/2.5/	1.260×10^{16}	0.0	77898.0	39
79	$CH_2O + M = CO + H_2 + M$ H_2O/16.25/CO/1.875/CO_2/3.75/CH_4/16.25/H_2/2.5/	2.80×10^{15}	0.0	63800.0	76
80	$CH_2O + HO_2 = HCO + H_2O_2$	1.000×10^{12}	0.0	8000	43
81	$CH_2O + OH = HCO + H_2O$	3.430×10^{9}	1.18	−447.0	41
82	$CH_2O + O = HCO + OH$	1.807×10^{13}	0.0	3088.0	41
83	$CH_2O + H = HCO + H_2$	2.300×10^{10}	1.05	3275	43
84	$CH_2O + O_2 = HCO + HO_2$	6.023×10^{13}	0.0	40699.8	39
85	$CH_2O + CH_3 = HCO + CH_4$	4.089×10^{12}	0.0	8851.6	39
86	$CH_3OH + OH = CH_3O + H_2O$	1.00×10^{6}	2.1	496.7	73
87	$CH_3OH + O = CH_2OH + OH$	1.630×10^{13}	0.0	5030.0	66
88	$CH_3OH + HO_2 = CH_2OH + H_2O_2$	9.64×10^{10}	0.0	12590.9	42
89	$CH_3OH + OH = CH_2OH + H_2O$	1.440×10^{6}	2.0	−840	43
90	$CH_3OH + H = CH_2OH + H_2$	1.700×10^{7}	2.1	4870	43
91	$CH_3O + CH_3O = CH_3OH + CH_2O$	6.023×10^{13}	0.0	0.0	41
92	$CH_3OH + CH_3 = CH_2OH + CH_4$	3.000×10^{7}	1.5	9940	43

Table 4. (Contd.)

No.	Reaction**	A	n	E	Reference
93	$CH_3OH + CH_3 = CH_3O + CH_4$	1.000×10^7	1.5	9940	43
94	$CH_3OH(+M) = CH_2OH + H(+M)$ Low/0.234×10^{41} -0.633×10^{1} 0.10310×10^{6}/ 0.10×10^{-9}/ TROE/0.773 0.693×10^{3} 0.5333×10^{4}	2.69×10^{16}	−0.1	98940.0	42
95	$CH_3OH + H = CH_3O + H_2$	3.60×10^{12}	0.0	6095	25
96	$CH_3OH + O_2 = CH_2OH + HO_2$	2.05×10^{13}	0.0	44900	42
97	$CH_3OH + HCO = CH_2OH + CH_2O$	9.63×10^3	2.90	13110	42
98	$CH_3OH + CH_3O = CH_3OH + CH_2OH$	3.00×10^{11}	0.0	4060	42
99	$CH_3OH(+M) = HCOH + H_2(+M)$ Low/5.02×10^{47} −8.402 94823./ TROE/0.9 615. 915. 4615./ H_2O/10.0/H_2/2.0/CO_2/3.0/ CO/2.0/	4.2×10^9	1.12	85604	64
100	$CH_3OH(+M) = CH_2O + H_2(+M)$ Low/9.784×10^{47} −8.4 101761./ TROE/0.9 825. 1125. 5700./ H_2O/10.0/ H_2/2.0/CO_2/3.0/CO/2.0/	2.03×10^9	1.0	91443	64
101	$CH_3OH + O_2 = HO_2 + CH_3O$	2.50×10^{12}	0.0	55000.0	76
102	$CH_3OH + M = CH_3 + OH + M$	3.50×10^{16}	0.0	66444.0	62
103	$CH_3OH + O = CH_3O + OH$	1.30×10^5	2.5	5000.0	43
104	$CH_2OH + M = CH_2O + H + M$ H_2O/16.25/ CO/1.875/CO_2/3.75/CH_4/16.25/	1.000×10^{14}	0.0	25100.0	57
105	$CH_2OH + H = CH_2O + H_2$	3.000×10^{13}	0.0	0.0	57
106	$CH_2OH + O_2 = CH_2O + HO_2$ (Deplicate)	2.168×10^{14}	0.0	4690.0	69
107	$CH_2OH + O_2 = CH_2O + HO_2$ (Deplicate)	1.51×10^{15}	−1.0	0.0	69
108	$CH_2OH + O = CH_2O + OH$	4.20×10^{13}	0.0	0.0	42
109	$CH_2OH + OH = CH_2O + H_2O$	2.40×10^{13}	0.0	0.0	42
110	$CH_2OH + HO_2 = HCOOH + OH + H$	2.00×10^{13}	0.0	0.0	41
111	$CH_2OH + HCO = CH_2O + CH_2O$	1.80×10^{14}	0.0	0.0	42
112	$CH_2OH + HO_2 = H_2O_2 + CH_2O$	4.00×10^{11}	0.0	0.0	76
113	$CH_2OH + HCO = CH_3OH + CO$	1.00×10^{13}	0.0	0.0	42
114	$CH_2OH + CH_3O = CH_3OH + CH_2O$	4.00×10^{12}	0.0	0.0	42
115	$CH_2OH + CH_2OH = CH_2O + CH_3OH$	4.00×10^{12}	0.0	0.0	42

Rate constants are given for direct reactions, $k = AT^n\exp(-E/RT)$ and the values E, n, A in this equation are expressed in cal, cm^3, mol, s; ** In reactions with "third body" (M) there are presented the efficiency of reactants (in square brackets). For representing some rate constant, we must give the parameters of the rate constant at low pressure (Low) and the formalism by which the software will calculate the rate at the high pressure. If the key word TROE is used this implies that "Chemkin" will use the Troe formalism for calculating the rate at high pressure.

In the case of flame I, the predominant channel is reaction 90, whereas reaction 87 contributes weakly to CH_2OH production (Table 5).

While formed, CH_2OH radical leads to the production of formaldehyde, mainly by the reaction 106 for flames (II and III) and by reactions 106 and 107 for the richest flame I:

(106) $CH_2OH + O_2 = CH_2O + HO_2$,

(107) $CH_2OH + O_2 = CH_2O + HO_2$.

This observation is in total accordance with that mentioned by Vandooren and Van Tiggelen [7], who reported that CH_2OH may disappear either with molecular oxygen or with other radicals such as M, H or O; however, as a consequence of the low mole fraction of CH_2OH and its high disappearance rate, the major reactant for CH_2OH should be molecular oxygen at least for the leanest flames (II and III).

b—CH_3O reactions

Regardless the flame composition, the methoxy radical (CH_3O) is mainly formed by methanol attack with OH and O (reactions 86 and 103). However, the reaction 103 is much less important in the case of flame I (Table 5):

(86) $CH_3OH + OH = CH_3O + H_2O$,

(103) $CH_3OH + O = CH_3O + OH$.

The radical CH_3O is then easily decomposed via a unimolecular reaction (reaction 70) to produce CH_2O and atomic hydrogen:

(70) $CH_3O + M = CH_2O + H + M$.

c—CH_2O reactions

As mentioned by Glarborg et al. [37], due to its importance in the oxidation of hydrocarbons and

Table 5. Maximum rates of the main elementary reactions evolved in CH_2OH, CH_3O, CH_2O for all the studied flames

Specie	Lean flames, Vandooren and Van Tiggelen flames											
	Flame I				Flame II				Flame III			
	Formation		Consumption		Formation		Consumption		Formation		Consumption	
	reaction	max rate	reaction	max rate	reaction	max rate	reaction	max rate	reaction	max rate	reaction	max rate
CH_2OH	87	1.31×10^{-5}	106	7.48×10^{-5}	87	1.31×10^{-5}	106	7.48×10^{-5}	87	1.66×10^{-5}	106	7.67×10^{-5}
	89	2.85×10^{-5}	107	1.7×10^{-6}	89	3.6×10^{-5}	107	1.7×10^{-6}	89	3.76×10^{-5}	107	1.78×10^{-6}
	90	3.6×10^{-5}	–	–	90	2.85×10^{-5}	–	–	90	2.52×10^{-5}	–	–
CH_3O	86	2.3×10^{-5}	70	2.88×10^{-5}	86	3.38×10^{-5}	70	4.42×10^{-5}	86	3.56×10^{-5}	70	4.7×10^{-5}
	103	5.45×10^{-6}	–	–	103	1.13×10^{-5}	–	–	103	1.48×10^{-5}	–	–
CH_2O	70	2.88×10^{-5}	81	7.33×10^{-5}	70	4.41×10^{-5}	81	9.66×10^{-5}	70	4.7×10^{-5}	81	9.77×10^{-5}
	106	8.66×10^{-5}	82	8.68×10^{-6}	106	7.48×10^{-5}	82	1.44×10^{-5}	106	7.67×10^{-5}	82	1.79×10^{-5}
	107	1.77×10^{-5}	83	3.99×10^{-5}	107	1.7×10^{-6}	83	1.42×10^{-5}	107	1.78×10^{-6}	83	1.2×10^{-5}

Specie	Stoichiometric flame, Pauwels' flame				Rich flame, Bradley's flame			
	Formation		Consumption		Formation		Consumption	
	reaction	max rate	reaction	max rate	reaction	max rate	reaction	max rate
CH_2OH	89	6.55×10^{-6}	106	2.99×10^{-5}	89	3.97×10^{-5}	104	2.14×10^{-5}
	90	2.44×10^{-5}	–	–	90	1.81×10^{-4}	106	1.91×10^{-4}
CH_3O	86	5.79×10^{-6}	70	7.54×10^{-6}	86	3.85×10^{-5}	70	4.95×10^{-5}
	95	8.05×10^{-7}	–	–	95	4.00×10^{-6}	–	–
	103	1.19×10^{-6}	–	–	103	8.57×10^{-6}	–	–
CH_2O	70	7.54×10^{-6}	81	2.70×10^{-5}	70	4.95×10^{-5}	81	1.23×10^{-4}
	106	2.99×10^{-5}	82	3.65×10^{-6}	104	2.14×10^{-5}	83	1.27×10^{-4}
	–	–	83	2.39×10^{-5}	106	1.91×10^{-4}	–	–

increasing concern about its emission, a detailed knowledge of the oxidation chemistry of formaldehyde is of significant practical interest. On the other hand, it is well known from the open literature that, this species originates mainly from CH_2OH (CH_3O) radical in a slightly exothermic step [7]. This finding is confirmed in our case, where we have found that the formaldehyde (CH_2OH) is produced either by bimolecular reaction of CH_2OH with molecular oxygen (reactions 106 and 107) or by the unimolecular decomposition of the methoxy radical (reaction 70). However, the contribution of reaction 107 to the CH_2O formation is negligible in the case of flames II and III (Table 5):

$$(106)\ CH_2OH + O_2 = CH_2O + HO_2,$$

$$(70)\ CH_3O + M = CH_2O + H + M,$$

$$(107)\ CH_2OH + O_2 = CH_2O + HO_2.$$

When formed, the formaldehyde CH_2O reacts with OH, H and O to form formic acid (HCO) via reactions 81, 83, and 82 for the three flames:

$$(81)\ CH_2O + OH = HCO + H_2O,$$

$$(83)\ CH_2O + H = HCO + H_2,$$

$$(82)\ CH_2O + O = HCO + OH.$$

The contribution of each reaction to the formaldehyde consumption is greatly influence by the flame composition and the H abstraction by OH is the predominant step.

Several rate constants' expressions of reactions 82 and 83 were proposed in the literature, in our study we have adopted the rate constants proposed by in the compilation of Tsang and Hampson [41]. On the other hand, the high temperature measurements of reaction 83 display significant scatter [37, 88]. We have chosen the constant proposed in the GRI mechanism [43].

Kinetic Analysis in Stoichiometric and Rich Flames

Fuel (CH_3OH) destruction. While the major paths of methanol consumption in lean flames were the H, O and OH attack leading to H abstraction, the main steps governing methanol decay in stoichiometric (flame of Pauwels, $\Phi = 1.08$) and rich (flame of Bradley, $\Phi = 1.25$) systems, involve thermal decomposition by reaction with H/OH radical pool (reactions 86, 89 and 90), whereas the O attack (reactions 87 and 103) becomes negligible. On the other hand, in contrary to

the lean flames (II and III), where the predominant step consuming methanol was the reaction between CH_3OH and OH, the most important step in the methanol consumption, in the case of stoichiometric and rich flames, was found to be the reaction between CH_3OH and H giving the radical hydroxymethyl. However, in all cases, the overall methanol consumption leads to the two isomers hydroxymethyl (CH_2OH) and methoxy (CH_3O) radicals. In the case of Pauwels' flame, the overall rate of methanol consumption leading to hydroxymethyl and methoxy radicals is evaluated to 84.23% (with a contribution of 66.41% for the H attack) and 15.76%, respectively, whereas in the case of Bradley's flame, it is evaluated to 85.14% (with a contribution of 69.83% for the H attack) and 14.85% for CH_2OH and CH_3O, respectively. These results are the consequence of the observed rise in H and OH concentrations upon increasing the equivalence ratio. The H and OH mole fractions in the flame of Bradley (2.09 and 3.02, respectively) are more important than the corresponding ones in the flame of Pauwels. These findings infer that the CH_2OH and CH_3O concentrations will be more important in the case of the flame of Bradley than the flame of Pauwels (the ratios of these two radicals in the two flames are 8.84 and 7.08, respectively) (Fig. 5).

Reactions of CH_2OH/CH_3O and CH_2O radicals. As in the case of lean flames, the most important intermediates from initial methanol oxidation, in stoichiometric and rich flames, are hydroxymethyl (CH_2OH) and methoxy (CH_3O) radicals. Thus, in these paragraphs, we will study in details the reactions governing formation and consumption of the two isomers.

a—CH_2OH reactions

The sensitivity analysis reveals that, regardless the flame equivalence ratio, the most important reactions in the hydroxymethyl radical formation are:

$$(89)\ CH_3OH + OH = CH_2OH + H_2O,$$
$$(90)\ CH_3OH + H = CH_2OH + H_2.$$

The reaction with H is the predominant one in the two flames. On the other hand, whatever the flame equivalence ratio, the hydroxymethyl radical decay is governed by the reaction with molecular oxygen (reaction 106), while the unimolecular decomposition of CH_2OH according to reaction 104 is only important in the case of rich flame (flame of Bradley).

b—CH_3O reactions

According to the sensitivity results, methanol thermal decomposition by reaction with OH/O/H radical pool (reactions 86, 95 and 103) is the main path in the production of the methoxy radical:

$$(86)\ CH_3OH + OH = CH_3O + H_2O,$$
$$(95)\ CH_3OH + H = CH_3O + H_2,$$
$$(103)\ CH_3OH + O = CH_3O + OH.$$

The contribution of each reaction in the methanol decay is dependent on the flame equivalence ratio. Abstraction by OH contributes with 74.37 and 75.39%, while the reaction with H contributes with 10.34 and 7.83%, and finally abstraction by O contributes with 15.28 and 16.78%o in the flames of Pauwels and Bradley, respectively. On the other hand, it is noteworthy that, whatever the flame equivalence ratio, the methoxy radical (CH_3O) is mainly consumed by its unimolecular decomposition (reaction 70) producing atomic hydrogen and formaldehyde (Table 5).

c—CH_2O reactions

It was above mentioned that, in the case of lean flames, the formaldehyde originates mainly from hydroxymethyl and methoxy radicals. Similar trends are observed in the case of stoichiometric and rich flames. In the case of the flame of Pauwels, formaldehyde (CH_2O) is produced either by bimolecular reaction of CH_2OH with molecular oxygen (reactions 106) or by the unimolecular decomposition of the methoxy radical (reactions 70), while in the case of the flame of Bradley, in addition to these reactions, formaldehyde is produced by the unimolecular decomposition of the hydroxymethyl radical (reactions 104):

$$(70)\ CH_3O + M = CH_2O + H + M,$$
$$(104)\ CH_2OH + M = CH_2O + H + M,$$
$$(106)\ CH_2OH + O_2 = CH_2O + HO_2.$$

The relative importance of the above reactions is dependent on the flame equivalence ratio. Reaction (70) contributes with 20.13 and 18.90%, whereas the contribution of the reaction (106) is evaluated to 79.86 and 72.93% for the flames of Pauwels and Bradley, respectively. Finally, it is noteworthy that the contribution of the reaction 104 in the case of the flame of Bradley suggests that the CH_2OH mole fraction, in this case, is large enough so that its reaction with molecular oxygen will be noticeable (8.16% of contribution, see Table 5).

On the other hand, the formaldehyde decay is found to be governed by three reactions in the case of the flame of Pauwels:

$$(81)\ CH_2O + OH = HCO + H_2O,$$
$$(82)\ CH_2O + O = HCO + OH,$$
$$(83)\ CH_2O + H = HCO + H_2.$$

with contributions evaluated to 49.50, 6.69 and 43.81% for reactions 81, 82 and 83, respectively. Whereas, in the case of the flame of Bradley, the formaldehyde consumption is essentially governed by the reactions 81 and 83. The first reaction contributes with 49.20%, while the second one exhibits a contribution of 50.80% (Table 5). These findings suggest that the increase in the equivalence ratio leads to the enhancement of the role of H and OH radicals and to the lowering of the role of atomic oxygen in the formaldehyde consumption.

CONCLUSION

A new detailed CH_3OH oxidation mechanism under flame conditions, featuring 21 species and 115 reactions, has been developed in a hierarchical manner by assembling selected reaction subsets from existing mechanisms for H_2, CO, CH_2O, and CH_3OH species. Evaluation of the detailed reaction mechanism has been carried out using three data sets encompassing different flames equivalence ratios. The data set of Vandooren and Van Tiggelen for the lean flames, those of Pauwels et al. for the stoichiometric flames and those of Bradley et al. for the rich flames. The computed CH_3OH, O_2, CO_2, H_2O, H, H_2, O, OH, CO, CH_2O and CH_3O (a combination of methoxy CH_3O and hydroxymethyl radicals CH_2OH) mole fractions, using the proposed model, were compared to those obtained by Held and Dryer, Egolfopolous and Pauwels models under the same conditions. The most outstanding observations are the next.

—The developed kinetic scheme has been shown to perform in a satisfactory manner under most situations. It displays a good to excellent agreements between predictions and measured mole fraction profiles for reactants, products, and intermediates species. The agreement between the computed and the experimental data is dependent on the flame equivalence ratio.

—Concerning CH_2O and CH_3O, which are very important intermediates in the methanol oxidation, the proposed model gives the best calculated values, as compared to the other used models, which demonstrate a huge discrepancy between detailed flame experiments and flame computations regarding the CH_3O maximum, especially for Pauwels model.

—Reaction path and analyses allow identification of important kinetic routes and reaction rates of selected species. While the major paths of methanol consumption in lean flames were the H, O and OH attack leading to H abstraction, the main steps governing methanol decay in stoichiometric and rich systems, involve thermal decomposition by reaction with H/OH radical pool (reactions 86, 89 and 90), whereas the 0 attack (reactions 87 and 103) becomes negligible. In contrary to the lean flames (II and III), where the predominant step consuming methanol was the reaction between CH_3OH and OH, the most important step in the methanol consumption, in the case of stoichiometric and rich flames, was found to be the reaction between CH_3OH and H giving the radical hydroxymethyl. However, in all cases, the overall methanol consumption leads to the two isomers hydroxymethyl (CH_2OH) and methoxy (CH_3O) radicals.

REFERENCES

1. Verma, S.S., *Energy Convers. Manage.*, 2002, vol. 43, p. 1999.
2. Cooke, D.F., Dodson, M.G., and Williams, A., *Combust. Flame*, 1971, vol. 16, p. 233.
3. Bowman, C.T., *Combust. Flame*, 1975, vol. 25, p. 343.
4. Tsuboi, T. and Hashimoto, K., *Combust. Flame*, 1981, vol. 42, p. 61.
5. Cribb, P.H., Dove, J.E., and Yamazaki, S., *Combust. Flame*, 1992, vol. 88, p. 186.
6. Singh, S., Grosshandler, W., Malte, P.C., and Crain, R.W., *Proc. Combust. Inst.,* 1979, vol. 17, p. 689.
7. Vandooren, J. and van Tiggelen, P.J., *Proc. Combust. Inst.*, 1981, vol. 18, p. 473.
8. Grotheer, H.H., Kelm, S., Driver, H.S.T., Hutcheon, R.J., Lockett, R.D., and Robertson, G.N., *Ber. Bunsen-Ges. Phys. Chem.*, 1992, vol. 96, p. 1360.
9. Grotheer, H.H. and Just, T., *Combust. Sci. Technol.*, 1993, vol. 91, p. 15.
10. Bell, K.M. and Tipper, C.F.H., *Trans. Faraday Soc.*, 1957, vol. 53, p. 982.
11. Norton, T.S. and Dryer, F.L., *Combust. Sci. Technol.*, 1989, vol. 63, p. 107.
12. Alzueta, M.U., Bilbao, R., and Finestra, M., *Energy Fuels*, 2001, vol. 15, p. 724.
13. Dayma, G., Ali, K.H., and Dagaut, P., *Proc. Combust. Inst.*, 2007, vol. 31, p. 411.
14. Rasmussen, C.L., Wassard, K.H., Johansen, K.D., and Glarborg, P., *Int. J. Chem. Kinet.*, 2008, vol. 40, p. 423.
15. Brock, E.E., Oshima, Y., Savage, P.E., and Barker, J.R., *J. Phys. Chem.*, 1996, vol. 100, p. 15834.
16. Anitescu, G., Zhang, Z., and Tavlarides, L.L., *Ind. Eng. Chem. Res.*, 1999, vol. 38, p. 2231.
17. Koda, S., Kanno, N., and Fujiwara, H., *Ind. Eng. Chem. Res.*, 2001, vol. 40, p. 3861.
18. Westbrook, C.K. and Dryer, F.L., *Combust. Sci. Technol.,* 1979, vol. 20, p. 125.
19. Dove, J.E. and Warnatz, J., *Ber. Bunsen-Ges. Phys. Chem.,* 1983, vol. 87, p. 1040.
20. Pauwels, J.F., Carlier, M., Devolder, P., and Sochet, L.R., *Combust. Sci. Technol.*, 1989, vol. 64, p. 97.
21. Egolfopoulos, F.N., Du, D.X., and Law, C.K., *Combust. Sci. Technol.*, 1992, vol. 83, p. 33.
22. Norton, T.S., *PhD Dissertation*, Princeton, N.J.: Princeton Univ., 1989.
23. Held, T.J. and Dryer, F.L., *Int. J. Chem. Kinet.*, 1998, vol. 30, p. 805.
24. Li, J., Zhao, Z., Kazakov, A., Chaos, M., Dryer, F.L., and Scire, J.J., *Int. J. Chem. Kinet.*, 2007, vol. 39, p. 109.
25. Held, T.J. and Dryer, F.L., *Proc. Combust. Inst.*, 1994, vol. 25, p. 901.
26. Lindstedt, R.P. and Meyer, M.P., *Proc. Combust. Inst.*, 2002, vol. 29, p. 1395.
27. Kee, R.J., Grcar, J.F., Smooke, M.D., and Miller, J.A., *A Fortran Program for Modelling Steady Laminar One-dimensional Premixed Flames: Sandia National Laboratories Rep. SAND*, 1985, p. 85.
28. Kee, R.J., Rupley, F.M., and Miller, J.A., *Chemkin II: A Fortran Chemical Kinetics Package for the Analysis of Gas Phase Chemical Kinetics. Sandia National Laboratories Rep. SAND*, 1989, p. 89.
29. Johnson, R.D. and Hudgens, J.W., *J. Phys. Chem.*, 1996, vol. 100, p. 19874.
30. Ruscic, B., Boggs, J.E., Burcat, A., Csaszar, A.G., Demaison, J., Janoschek, R., Martin, J.M.L., Morton, M.L., Rossi, M.J., Stanton, J.F., Szalay, P.G., Westmoreland, P.R., Zabel, F., and Berces, T., *J. Phys. Chem. Ref. Data*, 2005, vol. 34, p. 573.

31. Gordon, S. and McBride, B.J., *NASA SP*, 1971, p. 273.
32. Kee, R.J., Rupley, F.M., and Miller, J.A., *Rep. No. SAND87–8215*, Sandia National Laboratories, 1991.
33. Bradley, D., Dixon-Lewis, G., El-Din, Habik, S., Kwa, L.K., and El-Sherif, S., *Combust. Flame*, 1991, vol. 85, p. 105.
34. Wen-Chiun, I., Sheng, C.Y., and Bozzelli, J.W., *Fuel Process. Technol.*, 2003, vol. 83, p. 111.
35. Warnatz, J., *Combustion Chemistry*, Gardiner, W.C., Jr., Ed., New York: Springer, 1984, p. 197.
36. Kristensen, P.G., Karll, B., Bendtsen, A.B., Glarborg, P., and Dam-Johansen, K., *Combust. Sci. Technol.,* 2000, vol. 157, p. 262.
37. Glarborg, P., Alzueta, M.U., Kjærgaard, K., and Dam-Johansen, K., *Combust. Flame*, 2003, vol. 132, p. 629.
38. Lamoureux, N., El-Bakali, A., Gasnot, L., Pauwels, J.F., and Desgroux, P., *Combust. Flame*, 2008, vol. 153, p. 186.
39. Baulch, D.L., Cobos, C.J., Cox, R.A., Esser, C., Frank, P., Just, Th., Kerr, J.A., Pilling, M.J., Troe, J., Walker, R.W., and Warnatz, J.J., *J. Phys. Chem. Ref. Data*, 1992, vol. 21, p. 411.
40. Baulch, D.L., Cobos, C.J., Cox, R.A., Frank, P., Hayman, G., Just, Th., Kerr, J.A., Murrells, T., Pilling, M.J., Troe, J., Walker, R.W., and Warnatz, J.J., *J. Phys. Chem. Ref. Data*, 1994, vol. 23, p. 847.
41. Tsang, W. and Hampson, R.F., *J. Phys. Chem. Ref. Data*, 1986, vol. 15, p. 1087.
42. Tsang, W., *J. Phys. Chem. Ref. Data*, 1987, vol. 16, p. 471.
43. Frenklach, M., Wang, H., Goldenberg, M., Smith, G.P., Golden, M.M., Bowman, C.T., Hanson, R.K., Gardiner, W.C., and Lissianski, V.V., *GRI-Mech*, 1995.
44. Mueller, M.A., Kim, T.J., Yetter, R.A., and Dryer, F.L., *Int. J. Chem. Kinet.*, 1999, vol. 31, p. 113.
45. Natarajan, K. and Roth, P., *Combust. Flame*, 1987, vol. 70, p. 267.
46. Timonen, R.S., Ratajczak, E., and Gutman, D., *J. Phys. Chem.*, 1987, vol. 91, p. 692.
47. Hippler, H., Troe, J., and Willner, J.J., *J. Chem. Phys.,* 1990, vol. 93, p. 1755.
48. Troe, J., *J. Phys. Chem.,* 1979, vol. 83, p. 114.
49. Glarborg, P., Alzueta, M.U., Kjargaard, K., and Dam-Johansen, K., *Combust. Flame*, 2003, vol. 132, p. 629.
50. Emdee, J.L., Brezinsky, K., and Glassman, I., *J. Phys. Chem.*, 1992, vol. 96, p. 2151.
51. Schatz, G.C., Wagner, A.F., and Dunning, T.H., *J. Phys. Chem.,* 1984, vol. 88, p. 221.
52. Scire, J.J., Yetter, R.A., and Dryer, F.L., *Int. J. Chem. Kinet.*, 2001, vol. 33, p. 75.
53. Li, J., *PhD Dissertation,* Prineceton, N.J.: Princeton Univ., 2004.
54. Mueller, M.A., *PhD Dissertation*, Prineceton, N.J.: Princeton Univ., 2000.
55. Wantuck, P.J., Oldenborg, R.C., Baughcum, S.L., and Winn, K.R., *J. Phys. Chem.*, 1987, vol. 91, p. 4653.
56. Wooldridge, M.S., Hanson, R.K., and Bowman, C.T., *Int. J. Chem. Kinet.*, 1994, vol. 26, p. 389.
57. Warnatz, J., *Combustion Chemistry*, Gardiner, W.C., Jr., Ed., New York: Springer, 1984, p. 204.
58. Miller, J.A. and Kee, R.J., *J. Phys. Chem.*, 1977, vol. 81, p. 2534.
59. Frenklach, M., Wang, H., and Rabinowitz, M.J., *Prog. Energy Combust. Sci.*, 1992, vol. 18, p. 47.
60. Michael, J.V. and Sutherland, J.W., *J. Phys. Chem.*, 1988, vol. 92, p. 3853.
61. Eskola, J. and Timonen, R.S., *Phys. Chem. Chem. Phys.*, 2003, vol. 5, p. 2557.
62. Zhang, H.Y. and Mckinnon, J.T., *Combust. Sci. Technol.*, 1995, vol. 107, p. 261.
63. Miller, J.A. and Melius, C.F., *Combust. Flame*, 1992, vol. 91, p. 21.
64. Marinov, N.M., Pitz, W.J., Westbrook, C.K., Vincitore, A.M., Castaldi, M.J., Senkan, S.M., and Melius, C.F., *Combust. Flame*, 1998, vol. 114, p. 192.
65. Hippler, H. and Troe, J., *Chem. Phys. Lett.*, 1992, vol. 192, p. 333.
66. Keil, G.D., Tanzawa, T., Skolnik, E.G., Klemm, R.B., and Michael, J.V., *J. Chem. Phys.*, 1981, vol. 75, p. 2693.
67. Cohen, N., *Int. J. Chem. Kinet.*, 1986, vol. 18, p. 59.
68. Dean, A.M. and Westmoreland, P.R., *Int. J. Chem. Kinet.*, 1987, vol. 19, p. 207.
69. Grotheer, H.H., Riekert, G., Walter, D., and Just, T., *J. Phys. Chem.*, 1988, vol. 92, p. 4028.
70. Cobos, C.J. and Troe, J.Z., *Z. Phys. Chem.*, 1990, vol. 167, p. 129.
71. Dean, A.M., *J. Phys. Chem.*, 1985, vol. 89, p. 4600.
72. De Avillez, PereiraR., Baulch, D.L., Pilling, M.J., Robertson, S.H., and Zeng, G., *J. Phys. Chem.*, 1997, vol. 101, p. 9681.
73. Bott, J.F. and Cohen, N., *Int. J. Chem. Kinet.*, 1991, vol. 23, p. 1075.
74. Page, M., Lin, M.C., He, Y., and Choudhury, T.K., *J. Phys. Chem.,* 1989, vol. 93, p. 4404.
75. Lim, K.P. and Michael, J.V., *J. Chem. Phys.*, 1993, vol. 98, p. 3919.
76. Dayma, G., Ali, K.H., and Dagaut, P., *Proc. Combust. Inst,* 2007, vol. 31, p. 411.
77. Campbell, I.M., McLaughlin, D.F., and Handy, B.J., *Chem. Phys. Lett.*, 1976, vol. 38, p. 362.
78. Barnes, I., Bastian, V., Becker, K.H., Fink, E.H., and Zabel, F., *Atmos. Environ.*, 1982, vol. 16, p. 545.
79. Pagsberg, P., Munk, J., Sillesen, A., and Anastasi, C., *Chem. Phys. Lett.*, 1988, vol. 146, p. 375.
80. McCaulley, J.A., Kelly, N., Golde, M.F., and Kaufman, F., *J. Phys. Chem.*, 1989, vol. 93, p. 1014.
81. Nelson, L., Rattigan, O., Neavyn, R., Sidebottom, H., Treacy, J., and Nielsen, O.J., *Int. J. Chem. Kinet.*, 1990, vol. 22, p. 1111.
82. Dillon, T.J., Holscher, D., Sivakumaran, V., Horowitz, A., and Crowley, J.N., *Phys. Chem. Chem. Phys.*, 2005, vol. 7, p. 349.
83. Srinivasan, N.K., Su, M.C., and Michael, J.V., *J. Phys. Chem.*, 2007, vol. 111, p. 3951.
84. Hagele, J., Lorenz, K., Rhasa, D., and Zellner, R., *Ber. Bunsen-Ges. Phys. Chem.*, 1983, vol. 87, p. 1023.
85. Meier, U., Grotheer, H.H., Riekert, G., and Just, T., *Ber. Bunsen-Ges. Phys. Chem.*, 1985, vol. 89, p. 325.
86. Wallington, T.J. and Kurylo, M.J., *Int. J. Chem. Kinet.*, 1987, vol. 19, p. 1015.
87. Hess, W.P. and Tully, F.P., *J. Phys. Chem.*, 1989, vol. 93, p. 1944.
88. Baulch, D.L., Cobos, C.J., Cox, R.A., Frank, P., Hayman, G., Just, Th., Kerr, J.A., Pilling, M.J., Troe, J., Walker, R.W., and Warnatz, J., *Combust. Flame*, 1994, vol. 98, p. 59.